

1  
2  
3  
4  
5  
6  
7  
8  
9  
10  
11  
12  
13  
14  
15  
16  
17  
18  
19  
20  
21  
22  
23  
24

## SUPPLEMENTARY MATERIAL

### **SUPPLEMENTARY METHODS:**

#### **Bacterial strains:**

*C difficile* DS1684 (ribotype 010, non-toxicogenic strain) was used for chemostat experiments and mouse experiments. *C difficile* DS1684, *C difficile* CD630 (ribotype 012, virulent multidrug resistant strain), *C difficile* R20291 (ribotype 027, a hypervirulent strain), *Bacteroides uniformis*, *Bacteroides vulgatus*, and *Clostridium scindens* (DSM 5676) were used in batch culture experiments. *C difficile* ribotype 027 is a common ribotype in Europe and North America,<sup>1-3</sup> while ribotype 012 is one of the common ribotypes in mainland China.<sup>4,5</sup> CD630 and R20291 are genetically and phenotypically well-characterised and are good representatives of their ribotypes.<sup>6</sup> *B uniformis* and *B vulgatus* were isolated from the stool of a healthy male in his 30's using fastidious anaerobe agar (Lab M, Heywood, UK) or nutrient agar (Sigma-Aldrich, St. Louis, USA), respectively.

#### **Chemostat model of CDI:**

The working volume of each vessel was 235 ml and the growth medium feed was set to a retention time of 21 hours.<sup>7,8</sup> The composition of the growth medium consisted of a mixture of both soluble and insoluble starches, amino acids, peptides, proteins, vitamins, trace elements, and porcine gastric mucin (type II).<sup>9</sup> To mimic the gut environment cultures were maintained at a temperature of 37°C and a pH of 6.8, were gently agitated, and kept anaerobic by sparging with oxygen-free nitrogen gas. Chemostat cultures were sampled daily from each vessel and vessels were operated for 54 days post-inoculation. Chemostat culture samples were aliquoted and stored at -80°C for DNA extraction and mass spectrometry analysis. For NMR analysis, fresh chemostat culture was centrifuged at 20,000 x g and 4°C for 10 minutes, and the supernatant was aliquoted and stored at -80°C.

25 **Design of chemostat experiments:**

26 We induced CDI in our chemostat gut model following a modified version of the methods previously  
27 described by Freeman and colleagues (**Table 1**).<sup>10</sup> Briefly, chemostat cultures were grown for 24 days  
28 without experimental manipulation to allow the communities to stabilise. After sampling vessels on day  
29 24 we added  $7.8 \times 10^6$  *C difficile* spores to each vessel to achieve an initial concentration of  $3.3 \times 10^4$   
30 spores/mL.<sup>11</sup> On day 25 we added another dose of  $7.8 \times 10^6$  *C difficile* spores to both vessels, and  
31 clindamycin was added to both vessels at a final concentration of 33.9 mg/L every 12 hours for 7 days  
32 (from days 25-31). After stopping clindamycin dosing chemostat cultures were left to grow for 10 days  
33 without experimental manipulation (days 32-42). This was done to allow the perturbed microbial  
34 communities to stabilise, so we could more easily determine which bacteria or metabolites were altered  
35 by FMT, and which bacteria or metabolites were able to recover after antibiotic treatment in the absence  
36 of FMT. After sampling on day 42 we added a single dose of saline to VA (control vessel) and a single dose  
37 of FMT to VB (test vessel). Chemostat cultures were then left to grow for a further 12 days without further  
38 experimental manipulation to monitor the effects of FMT on the chemostat communities (days 43-54).

39

40 ***C difficile* spore preparation:**

41 *C difficile* spores were prepared using previously described methods.<sup>11</sup> *C difficile* DS1684 was grown  
42 anaerobically on fastidious agar plates supplemented with 5% defibrinated horse blood (VWR, Radnor,  
43 USA) and incubated at 37°C for 7 days. The growth was removed from the plates using a sterile loop and  
44 resuspended in 1 mL sterile water. Next, 1 mL of 95% ethanol was mixed with the cell suspension and was  
45 incubated for 1 hour at room temperature. The cell suspension was then centrifuged at 3000 x g and  
46 resuspended in 1 mL sterile water. Spores were enumerated by preparing serial 10-fold dilutions in  
47 phosphate buffered saline (PBS) (Sigma-Aldrich) and plating the dilutions on Braziers Cycloserine,  
48 Cefoxitin Egg Yolk agar plates (containing Braziers CCEY agar base (Lab M), 250 mg/L cycloserine (VWR), 8

49 mg/L cefoxitin (Sigma-Aldrich), 8% egg yolk emulsion (SLS, Nottingham UK), 2% lysed defibrinated horse  
50 blood (VWR), and 5 mg/L lysozyme (Sigma-Aldrich)).<sup>12</sup> Plates were incubated anaerobically at 37°C for 48  
51 hours and the number of colonies were enumerated.

52

### 53 **Enumeration of *C difficile* counts from chemostat culture samples:**

54 *C difficile* total viable counts and spore counts were quantified from fresh chemostat culture samples  
55 every other day starting 26 days post-inoculation. *C difficile* total viable counts (TVC) were enumerated  
56 from fresh chemostat culture samples by performing serial 10-fold dilutions in PBS and plating onto  
57 Brazier's Cycloserine, Cefoxitin Egg Yolk agar plates (as described above, with the addition of 2 mg/L  
58 moxifloxacin (VWR)) in triplicate using the Miles and Misra method.<sup>13</sup> *C difficile* spore counts were  
59 enumerated from alcohol-shocked chemostat culture samples by mixing an equal volume of fresh  
60 chemostat culture sample with 95% ethanol and incubating at room temperature for one hour. Samples  
61 were then centrifuged at 3000 x g and 4°C for 10 minutes and resuspended in PBS. Spores were then  
62 quantified by performing serial 10-fold dilutions in PBS and plating onto Brazier's Cycloserine, Cefoxitin  
63 Egg Yolk agar plates (as described above, without the addition of moxifloxacin) in triplicate using the Miles  
64 and Misra method. Plates were incubated anaerobically at 37°C for two days and colonies were  
65 enumerated.

66

### 67 **Preparation and instillation of FMT:**

68 Fresh faecal samples were placed into an anaerobic chamber within 5 minutes of defecation. FMT  
69 preparations were prepared by homogenising 10 g of stool in 100 mL of anaerobic 0.9% saline in a strainer  
70 stomacher bag (250 rpm for 1 min). We added 50 mL of anaerobic saline to VA (control vessel) and 50 mL  
71 of homogenised stool to VB (test vessel). For Run 1 and Run 2 the stool transplant was prepared from the  
72 stool of a healthy male donor in his 30's, and for Run 3 the stool transplant was prepared from the stool

73 of a healthy female donor in her 20's. Both individuals have been used as FMT donors to treat CDI patients  
74 in Imperial's FMT Programme (and therefore undergone the appropriate donor screening protocols), and  
75 had not taken antibiotics for at least 3 months prior to providing the stool sample.

76

#### 77 **DNA extraction:**

78 DNA was extracted from 250 µL of chemostat culture using the PowerLyzer PowerSoil DNA Isolation  
79 Kit (Mo Bio, Carlsbad, USA) following the manufacturer's protocol, except that samples were lysed by  
80 bead beating for 3 min at speed 8 using a Bullet Blender Storm instrument (Chembio Ltd, St. Albans, UK).  
81 DNA was aliquoted and stored at -80°C until it was ready to be used.

82

#### 83 **16S rRNA gene qPCR:**

84 16S rRNA gene qPCR data was used to determine the total bacterial biomass within each sample and  
85 was performed using extracted chemostat culture DNA to following a previously published protocol.<sup>14</sup> A  
86 total volume of 20 µL was used for each reaction and consisted of the following: 1x Platinum Supermix  
87 with ROX (Life Technologies, Carlsbad, USA), 1.8 µM BactQUANT forward primer (5'-  
88 CCTACGGGAGGCAGCA-3'), 1.8 µM BactQUANT reverse primer (5'-GGACTACGGGTATCTAATC-3'), 225 nM  
89 probe ((6FAM) 5'-CAGCAGCCGCGGTA-3' (MGBNFQ)), PCR grade water (Roche, Penzberg, Germany), and  
90 5 µL DNA. Each PCR plate included a standard curve using *E. coli* DNA (Sigma-Aldrich) (3-300,000 copies  
91 per reaction in 10-fold serial dilutions) as well as no template negative controls. All samples, standards,  
92 and controls were amplified in triplicate. Extracted DNA samples were diluted to ensure they fell within  
93 the standard curve. Amplification and real-time fluorescence detections were performed using the  
94 Applied Biosystems StepOnePlus Real-Time PCR System using the following PCR cycling conditions: 50 °C  
95 for 3 min, 95 °C for 10 min, and 40 cycles of 95 °C for 15 sec and 60 °C for 1 min. We used a paired t-test

96 to compare changes in log-transformed 16S rRNA gene copy number between samples at specific time  
97 points.

98

#### 99 **Pre-processing and analysis of 16S rRNA gene sequencing data:**

100 We used the Mothur package (v1.35.1) to preprocess and analyse the resulting sequencing data  
101 following the MiSeq SOP Pipeline.<sup>15</sup> We used the Silva bacterial database for sequence alignments  
102 ([www.arb-silva.de/](http://www.arb-silva.de/)) and the RDP database reference sequence files for classification of sequences using  
103 the Wang method.<sup>16</sup> We determined the Operational Taxonomic Unit (OTU) taxonomies (phylum to  
104 genus) using the RDP MultiClassifier script. We resampled and normalised data to the lowest read count  
105 in Mothur (9527 reads per sample), which resulted in greater than 99.4% coverage within each sample.  
106 We used 16S rRNA gene qPCR data and the following formula to express our 16S rRNA gene sequencing  
107 data as absolute abundances (instead of relative abundances):

108 *Absolute abundance of taxa*

$$109 = \text{relative abundance of taxa} \times \left( \frac{\text{16S rRNA gene copy number in sample}}{\text{highest 16S rRNA gene copy number in sample set}} \right)$$

110 The Shannon diversity index ( $H'$ ), Pielou evenness index ( $J'$ ), and richness (total number of bacterial  
111 taxa observed,  $S_{\text{obs}}$ ) were calculated using the vegan library<sup>17</sup> within the R statistical package.<sup>18</sup>

112 Stream plots were prepared by plotting the absolute abundance of 16S rRNA gene sequencing data  
113 (biomass-corrected) over time (OTU-level, coloured by phylum). This was accomplished using the  
114 streamgraph function within the streamgraph library (v0.8.1) within R.<sup>19</sup>

115

#### 116 **<sup>1</sup>H-NMR spectroscopy sample preparation:**

117 Chemostat culture supernatants were randomized and defrosted at room temperature for 1 hour.  
118 Once samples were defrosted supernatants were centrifuged at 20,000 x g and 4°C for 10 minutes. Next,  
119 400 µL of chemostat culture supernatant was mixed with 250 µL of sodium phosphate buffer solution

120 (28.85 g Na<sub>2</sub>HPO<sub>4</sub> (Sigma-Aldrich), 5.25 g NaH<sub>2</sub>PO<sub>4</sub> (Sigma-Aldrich), 1 mM TSP (Sigma-Aldrich), 3 mM NaN<sub>3</sub>  
121 (Sigma-Aldrich), deuterium oxide (Goss Scientific Instruments, Crewe, UK) to 1 L, pH 7.4)<sup>20</sup> and 600 µL was  
122 pipetted into a 5 mm NMR tube.

123

#### 124 **Confirmation of NMR metabolite identities using 1D-NMR with spike-in and 2D-NMR spectroscopy:**

125 We used the statistical total correlation spectroscopy (STOCSY) analysis method to aid in the  
126 identification of metabolites in NMR spectra by determining correlations between intensities of the  
127 various peaks across the whole sample.<sup>21</sup> To further confirm if the peaks assigned to valerate and other  
128 metabolites were correct, we also conducted a two-dimensional NMR spectra (including <sup>1</sup>H-<sup>1</sup>H TOCSY and  
129 <sup>1</sup>H-<sup>1</sup>H COSY) for the chemostat culture supernatant and valerate standard using typical parameters to  
130 confirm the connectivity of the proton in the metabolites.<sup>22,23</sup>

131 For the valerate spike-in experiment one-dimensional <sup>1</sup>H NMR spectra were acquired as described in  
132 the <sup>1</sup>H-NMR spectroscopy methods section from the main text, except 64 scans were recorded into 65536  
133 data points with a spectral width of 20 ppm. After normal 1D <sup>1</sup>H NOESY NMR acquisition, 10 µL of valerate  
134 standard (99%, 0.9 M in PBS buffer) (Fisher Scientific, Hampton, USA) was added into the sample. A one-  
135 dimensional spectrum was recorded again to see if the relevant peaks of valerate increased.

136

#### 137 **Data pre-processing and analysis of UPLC-MS bile acid data:**

138 Quality control samples were prepared using a mixture of equal parts of the chemostat culture  
139 supernatants. We used the quality control samples as an assay performance monitor and to guide the  
140 removal of features with high variation.<sup>24</sup> We also spiked quality control samples with defined mixtures  
141 of bile acids to determine the chromatographic retention times of specific bile acids and to aid in  
142 metabolite identification (55 bile acid standards, including 36 non-conjugated bile acids, 12 tauro-  
143 conjugated bile acids, and 7 glyco-conjugated bile acids) (Steraloids, Newport, USA).

144 We converted the Waters raw data files to NetCDF format and extracted the data using XCMS (v1.50)  
145 package implemented within the R (v3.3.1) software. Dilution effects were corrected for using  
146 probabilistic quotient normalisation<sup>25</sup> and chromatographic features with high coefficient of variation  
147 (higher than 30% in the quality control samples) were excluded from further analysis.

148

#### 149 **Short Asynchronous Time-series Analysis (SANTA):**

150 SANTA is an automated pipeline that is implemented within R and controlled through a graphical user  
151 interface developed with Shiny.<sup>26,27</sup> This method analyses short time series by estimating trajectories as  
152 a smooth spline, and calculates whether time trajectories are significantly altered between different  
153 groups or over different time periods. SANTA was used to make the following comparisons: stabilisation  
154 period vs. clindamycin-dosing period, stabilisation period vs. post-clindamycin stabilisation period, and  
155 FMT-treated vs. saline-treated cultures during the treatment period. We used mean subtraction to  
156 eliminate between-run differences in metabolite concentrations that arose from differences in the stool  
157 used to seed the chemostat vessels. For each metabolite, we calculated the mean for all samples within  
158 the same chemostat run, then we subtracted the mean from all its values within the run.<sup>28</sup> Depending  
159 upon the time series being analysed, the number of degrees of freedom (df) to fit the spline model was  
160 chosen to avoid overfitting the data (df = 3-5). We report the  $p_{\text{Dist}}$  values, which uses the area between  
161 the mean group fitted curves to determine whether there is a difference between the two groups over  
162 time. Analysis used 1000 permutation rounds to calculate p-values and 1000 bootstrap rounds to calculate  
163 the 95% confidence bands. Reported  $p_{\text{Dist}}$  values are with Benjamini-Hochberg FDR correction, and  $p <$   
164 0.05 was considered significant.

165

#### 166 **Integration of 16S rRNA gene sequencing data and metabolite data:**

167 We used regularised Canonical Correlation Analysis (rCCA) to correlate 16S rRNA gene sequencing data  
168 (genus level) with bile acid mass spectrometry or <sup>1</sup>H-NMR data from the same set of samples using the  
169 mixOmics library within R.<sup>29</sup> rCCA is an unsupervised method that maximises the correlation between the  
170 two data sets X and Y (information on the treatment groups is not taken into account in the analysis). We  
171 used the shrinkage method to determine the regularisation parameters. The plotIndiv function was used  
172 to generate unit representation plots, where each point on the scatter plot represents a single chemostat  
173 culture sample, and samples were projected into the XY-variate space. The plotVar function was used to  
174 generate correlation circle plots, where strong correlations between variables (correlations greater than  
175 0.5) are plotted outside of the inner circle. Variables are represented through their projections onto the  
176 planes defined by their respective canonical variates. In this plot the variables projected in the same  
177 direction from the origin have a strong positive correlation, and variables projected in opposite directions  
178 from the origin have strong negative correlations. Variables with stronger correlations sit at farther  
179 distances from the origin.

180

#### 181 ***C. difficile* germination batch cultures with taurocholic acid (TCA):**

182 To test the effects of TCA on *C. difficile* germination we resuspended *C. difficile* DS1684 spores in  
183 supplemented brain heart infusion broth with or without 1% TCA (Sigma-Aldrich) in triplicate.<sup>30</sup> The OD<sub>600</sub>  
184 was measured immediately after inoculation of broths (time zero) and after an overnight incubation at  
185 37°C in anaerobic chamber. A paired t-test was used to determine whether TCA affected *C. difficile*  
186 germination.

187

#### 188 ***C. difficile* vegetative growth batch cultures with TCA:**

189 To test the effects of TCA on *C. difficile* vegetative growth we centrifuged an overnight culture of *C.*  
190 *difficile* DS1684 at 3000 x g for 10 minutes and resuspended the cells in supplemented brain heart infusion



191 broth with or without 1% TCA (in triplicate). The OD<sub>600</sub> was measured at time zero and cultures were  
192 incubated at 37°C in an anaerobic chamber. Additional OD<sub>600</sub> measurements were taken at 2, 4, 6, and 8  
193 hours post-inoculation, and the change in OD<sub>600</sub> was plotted against time. A paired t-test was used to  
194 determine whether TCA affected vegetative growth during the exponential phase.

195

#### 196 **SUPPLEMENTARY RESULTS:**

##### 197 ***C. difficile* total viable counts and spore counts:**

198 There was no significant difference in *C. difficile* TVC at the end of the clindamycin-dosing period  
199 compared to TVC immediately prior to administering FMT or saline treatment ( $p>0.05$ ). There was also no  
200 significant difference in *C. difficile* TVC in vessels assigned to receive FMT or saline treatment immediately  
201 prior to administering the treatment ( $p>0.05$ ).

202

##### 203 **<sup>1</sup>H-NMR spectroscopy:**

204 Following FMT or saline treatment there were significant strong negative correlations between  
205 valerate and 5-aminovalerate ( $r_s=-0.76$ ,  $p=5.27\times 10^{-6}$ ), ethanol ( $r_s=-0.69$ ,  $p=6.53\times 10^{-5}$ ), and methanol ( $r_s=-$   
206  $0.78$ ,  $p=3.11\times 10^{-6}$ ).

207

##### 208 **Confirmation of valerate in chemostat culture supernatant by 1D- and 2D-NMR:**

209 The chemical shifts for the 1D <sup>1</sup>H-NMR spectrum of 99% valerate standard were: 0.9 (t), 1.3 (dt), 1.46  
210 (m), 2.2 (t) (**Figure S5A**). Overlay of the 1D <sup>1</sup>H-NMR spectrum of the valerate standard with the sample  
211 showed that each peak of the valerate standard is visible in the sample (**Figure S5B**). Overlay of 1D <sup>1</sup>H-  
212 NMR spectra of the sample before and after valerate spike-in showed that all the valerate peaks increased  
213 after spike-in (**Figure S5C**). For 2D-NMR analysis overlay of the <sup>1</sup>H-<sup>1</sup>H COSY spectrum of the valerate  
214 standard with the sample showed that each peak of the valerate standard was present in the sample

215 spectrum (**Figure S6A**). Overlay of  $^1\text{H}$ - $^1\text{H}$  TOCSY spectrum of the valerate standard with the sample showed  
216 that each peak of the valerate standard was present in the sample spectrum (**Figure S6B**).

217

#### 218 **SUPPLEMENTARY DISCUSSION:**

219 Valerate is not expected to be harmful to host gut cells, as exposure of gut organoids to 5 mM valerate  
220 did not result in cell death or cause significant alterations in gene expression (Drs. Lee Parry and Richard  
221 Brown of the European Cancer Stem Cell Research Institute, personal communication, 19 Dec. 2017).  
222 Moreover, mice that received 15 mM glycerol trivalerate in our study did not show any adverse reactions.

223 The bacterial enzyme 7- $\alpha$ -dehydroxylase is responsible for converting unconjugated primary bile acids  
224 CA and CDCA to the secondary bile acids DCA and LCA, respectively. DCA and LCA have been shown to  
225 inhibit *C difficile* vegetative growth at specific concentrations,<sup>30,31</sup> and a previous study has shown that  
226 DCA and LCA were depleted in pre-FMT samples from recurrent CDI patients, but were restored in post-  
227 FMT samples.<sup>32</sup> These findings led researchers to propose antibiotic exposure results in the loss of bacteria  
228 with 7- $\alpha$ -dehydroxylase activity, reducing DCA and LCA production and permitting *C difficile* vegetative  
229 growth. A study by Buffie and colleagues found that administration of *Clostridium scindens* (a bacterium  
230 with 7- $\alpha$ -dehydroxylase activity) was associated with resistance to *C difficile* by restoring the production  
231 of the secondary bile acids DCA and LCA.<sup>33</sup> However, in our study we found that the levels of DCA and LCA  
232 recovered in chemostat cultures following the cessation of clindamycin. While we did find strong negative  
233 correlations between *C difficile* TVC and the secondary bile acids DCA and LCA, recovery of these bile acids  
234 to pre-clindamycin levels was not enough to decrease vegetative *C difficile* counts in chemostat cultures.  
235 Indeed, while DCA can inhibit *C difficile* vegetative growth, it appears that DCA can also encourage spore  
236 germination at specified concentrations.<sup>30</sup> A better strategy to prevent CDI prior to antibiotic exposure  
237 would be to prevent germination altogether by degrading TCA, a potent pro-germinant, using bile salt  
238 hydrolase enzymes.

239 Our chemostat experiments more closely modelled the first episode of CDI and not recurrent CDI. In  
240 first episodes of CDI, human patients are exposed to *C difficile* spores while taking an inciting antibiotic  
241 (e.g. clindamycin). In our study clindamycin exposure was sufficient to deplete valerate and elevate levels  
242 of TCA, allowing *C difficile* spore germination and vegetative growth. We waited 10 days after stopping  
243 clindamycin dosing before administering the FMT preparation to allow the perturbed microbial  
244 communities to stabilise following the cessation of antibiotics. This delay allowed us to more easily  
245 determine which metabolites were altered only by FMT, and which metabolites were able to recover after  
246 antibiotic treatment (in the absence of FMT). This feature is a major advantage of performing chemostat  
247 studies, as it would be unethical to withhold treatment from recurrent CDI patients in human studies to  
248 determine which metabolites would recover in the absence of FMT. We found no significant difference in  
249 *C difficile* TVC at the end of the clindamycin-dosing period compared to TVC immediately prior to  
250 administering FMT or saline treatment (see Supplementary Results). This means the metabolites that  
251 recovered following the cessation of clindamycin dosing, but before FMT, did not affect the vegetative  
252 growth of *C difficile* (i.e. bile acids). However, we did see a significant decrease in *C difficile* TVC and spore  
253 counts after FMT. This decrease suggests that bacterial metabolites that decreased *C difficile* counts did  
254 not recover after stopping clindamycin, but only recovered with FMT (i.e. valerate).

255 Most human studies of CDI have focused on recurrent CDI, not first episode of CDI. In this study we  
256 showed that valerate was depleted in recurrent CDI patients pre-FMT, but was restored post-FMT. To our  
257 knowledge this is the first study to measure valerate in the stool of recurrent CDI patients pre- and post-  
258 FMT. A previous study by Weingarden and colleagues found that TCA was elevated in the stool of  
259 recurrent CDI patients pre-FMT, but was decreased post-FMT.<sup>32</sup> It is important to note that in these human  
260 studies recurrent CDI patients were taking vancomycin when pre-FMT samples were collected, and FMT  
261 was administered to recurrent CDI patients within 1-2 days of stopping vancomycin therapy. While we  
262 could have designed our chemostat experiments to also include a vancomycin dosing regimen, followed

263 by FMT administration 1-2 days later, broad-spectrum vancomycin therapy would have killed more gut  
264 bacteria and depleted the chemostat cultures of additional ecosystem functions that were not important  
265 for the establishment of the infection, leading to false positives once these functionalities were restored  
266 following FMT. In our chemostat experiments FMT was administered 10 days after stopping clindamycin  
267 and pre-FMT samples were collected immediately prior to FMT administration. Had we chosen to  
268 administer the FMT preparation within 1-2 days after stopping clindamycin we would expect TCA levels  
269 to decrease with FMT.

270

271 **REFERENCES:**

- 272 1. Wilcox MH, Shetty N, Fawley WN, *et al.* Changing epidemiology of *Clostridium difficile* infection  
273 following the introduction of a national ribotyping-based surveillance scheme in England. Clin Infect  
274 Dis 2012;55:1056-1063.
- 275 2. Waslawski S, Lo ES, Ewing SA, *et al.* *Clostridium difficile* ribotype diversity at six health care institutions  
276 in the United States. J Clin Microbiol 2013;51:1938-1941.
- 277 3. Davies KA, Longshaw CM, Davis GL, *et al.* Underdiagnosis of *Clostridium difficile* across Europe: the  
278 European, multicentre, prospective, biannual, point-prevalence study of *Clostridium difficile* infection  
279 in hospitalised patients with diarrhoea (EUCLID). Lancet Infect Dis 2014;14:1208-1219.
- 280 4. Huang H, Fang H, Weintraub A, *et al.* Distinct ribotypes and rates of antimicrobial drug resistance in  
281 *Clostridium difficile* from Shanghai and Stockholm. Clin Microbiol Infect 2009;15:1170-1173.
- 282 5. Hawkey PM, Marriott C, Liu WE, *et al.* Molecular epidemiology of *Clostridium difficile* infection in a  
283 major Chinese hospital: an underrecognized problem in Asia? J Clin Microbiol 2013;51:3308-3313.
- 284 6. Dawson LF, Valiente E, Donahue EH, *et al.* Hypervirulent *Clostridium difficile* PCR-ribotypes exhibit  
285 resistance to widely used disinfectants. PLoS One 2011;6:e25754.

- 286 7. Allison C, McFarlan C, MacFarlane GT. Studies on mixed populations of human intestinal bacteria grown  
287 in single-stage and multistage continuous culture systems. *Appl Environ Microbiol* 1989;55:672-678.
- 288 8. Duncan SH, Scott KP, Ramsay AG, *et al.* Effects of alternative dietary substrates on competition between  
289 human colonic bacteria in an anaerobic fermentor system. *Appl Environ Microbiol* 2003;69:1136-1142.
- 290 9. McDonald JA, Schroeter K, Fuentes S, *et al.* Evaluation of microbial community reproducibility, stability  
291 and composition in a human distal gut chemostat model. *J Microbiol Methods* 2013;95:167-174.
- 292 10. Freeman J, Baines SD, Saxton K, *et al.* Effect of metronidazole on growth and toxin production by  
293 epidemic *Clostridium difficile* PCR ribotypes 001 and 027 in a human gut model. *J Antimicrob*  
294 *Chemother* 2007;60:83-91.
- 295 11. Freeman J, O'Neill FJ, Wilcox MH. Effects of cefotaxime and desacetylcefotaxime upon *Clostridium*  
296 *difficile* proliferation and toxin production in a triple-stage chemostat model of the human gut. *J*  
297 *Antimicrob Chemother* 2003;52:96-102.
- 298 12. Crowther GS, Chilton CH, Todhunter SL, *et al.* Comparison of planktonic and biofilm-associated  
299 communities of *Clostridium difficile* and indigenous gut microbiota in a triple-stage chemostat gut  
300 model. *J Antimicrob Chemother* 2014;69:2137-2147.
- 301 13. Miles AA, Misra SS, Irwin JO. The estimation of the bactericidal power of the blood. *J Hyg (Lond)*  
302 1938;38:732-749.
- 303 14. Liu CM, Aziz M, Kachur S, *et al.* BactQuant: an enhanced broad-coverage bacterial quantitative real-  
304 time PCR assay. *BMC Microbiol* 2012;12:56-2180-12-56.
- 305 15. Kozich JJ, Westcott SL, Baxter NT, *et al.* Development of a dual-index sequencing strategy and curation  
306 pipeline for analyzing amplicon sequence data on the MiSeq Illumina sequencing platform. *Appl*  
307 *Environ Microbiol* 2013;79:5112-5120.
- 308 16. Wang Q, Garrity GM, Tiedje JM, *et al.* Naive Bayesian classifier for rapid assignment of rRNA sequences  
309 into the new bacterial taxonomy. *Appl Environ Microbiol* 2007;73:5261-5267.

- 310 17. Oksanen J, Blanchet FG, Friendly M, *et al.* vegan: Community Ecology Package. R package version 2.4-  
311 3.; 2017. Available at: <https://CRAN.R-project.org/package=vegan>, 2017.
- 312 18. R Core Team. R: A language and environment for statistical computing. R Foundation for Statistical  
313 Computing, Vienna, Austria.; 2015. Available at: <https://www.R-project.org/>, 2017.
- 314 19. Rudis B. streamgraph: streamgraph is an htmlwidget for building streamgraph visualizations. R  
315 package version 0.8.1.; 2015. Available at: <http://github.com/hrbrmstr/streamgraph>, 2017.
- 316 20. Beckonert O, Keun HC, Ebbels TM, *et al.* Metabolic profiling, metabolomic and metabonomic  
317 procedures for NMR spectroscopy of urine, plasma, serum and tissue extracts. Nat Protoc  
318 2007;2:2692-2703.
- 319 21. Cloarec O, Dumas ME, Craig A, *et al.* Statistical total correlation spectroscopy: an exploratory approach  
320 for latent biomarker identification from metabolic <sup>1</sup>H NMR data sets. Anal Chem 2005;77:1282-1289.
- 321 22. Liu Z, Wang L, Zhang L, *et al.* Metabolic Characteristics of 16HBE and A549 Cells Exposed to Different  
322 Surface Modified Gold Nanorods. Adv Healthc Mater 2016;5:2363-2375.
- 323 23. Dai H, Xiao C, Liu H, *et al.* Combined NMR and LC-DAD-MS analysis reveals comprehensive  
324 metabonomic variations for three phenotypic cultivars of Salvia Miltiorrhiza Bunge. J Proteome Res  
325 2010;9:1565-1578.
- 326 24. Sangster T, Major H, Plumb R, *et al.* A pragmatic and readily implemented quality control strategy for  
327 HPLC-MS and GC-MS-based metabonomic analysis. Analyst 2006;131:1075-1078.
- 328 25. Veselkov KA, Vingara LK, Masson P, *et al.* Optimized preprocessing of ultra-performance liquid  
329 chromatography/mass spectrometry urinary metabolic profiles for improved information recovery.  
330 Anal Chem 2011;83:5864-5872.
- 331 26. Chang W, Cheng J, Allaire JJ, *et al.* shiny: Web Application Framework for R. R package version 1.0.3.;  
332 2017. Available at: <https://CRAN.R-project.org/package=shiny>, 2017.

- 333 27. Wolfer A. SANTA-App: Interactive package for Short Asynchronous Time-series Analysis (SANTA) in R,  
334 implemented in Shiny; 2017. Available at: <https://github.com/adwolfer/SANTA-App>, 2017.
- 335 28. **Gratton J, Phetcharaburanin J**, Mullish BH, *et al.* Optimized Sample Handling Strategy for Metabolic  
336 Profiling of Human Feces. *Anal Chem* 2016;88:4661-4668.
- 337 29. Le Cao K, Rohart F, Gonzalez I, *et al.* mixOmics: Omics Data Integration Project. R package version  
338 6.1.2.; 2017. Available at: <https://CRAN.R-project.org/package=mixOmics>, 2017.
- 339 30. Sorg JA, Sonenshein AL. Bile salts and glycine as cogerminants for *Clostridium difficile* spores. *J*  
340 *Bacteriol* 2008;190:2505-2512.
- 341 31. Thanissery R, Winston JA, Theriot CM. Inhibition of spore germination, growth, and toxin activity of  
342 clinically relevant *C difficile* strains by gut microbiota derived secondary bile acids. *Anaerobe*  
343 2017;45:86-100.
- 344 32. **Weingarden AR, Chen C**, Bobr A, *et al.* Microbiota transplantation restores normal fecal bile acid  
345 composition in recurrent *Clostridium difficile* infection. *Am J Physiol Gastrointest Liver Physiol*  
346 2014;306:G310-9.
- 347 33. Buffie CG, Bucci V, Stein RR, *et al.* Precision microbiome reconstitution restores bile acid mediated  
348 resistance to *Clostridium difficile*. *Nature* 2015;517:205-208.

349

350 **Author names in bold designate shared co-first authorship**

351

#### 352 **SUPPLEMENTARY FIGURE LEGENDS:**

353 **Figure S1:** Stream plots showing the OTU abundances in each chemostat culture over time. Each stream  
354 of colour represents an OTU, and streams are grouped by phylum: *Bacteroidetes* (blue), *Firmicutes*  
355 (green), *Proteobacteria* (orange), *Verrucomicrobia* (purple), unclassified (grey), and *C difficile* (red). The

356 width of the stream represents the OTU abundance at each time point. The dotted box indicates the  
357 clindamycin-dosing period, while the dotted vertical line indicates the day of FMT or saline dosing.

358 **Figure S2:** Diversity of bacterial communities cultured in chemostat vessels (VA= saline-treated cultures,  
359 dashed line; VB= FMT-treated cultures, solid line). **(A)** Shannon diversity index ( $H'$ ), **(B)** Richness ( $S_{obs}$ ), **(C)**  
360 Pielou's evenness index ( $J'$ ). The shaded grey box indicates the clindamycin-dosing period, while the  
361 vertical dotted line indicates the day of FMT or saline dosing. SANTA analysis with Benjamini-Hochberg  
362 FDR was used to compare the following: steady state cultures to clindamycin-treated cultures, steady  
363 state cultures to post-clindamycin cultures, and FMT-treated cultures to saline treated cultures.

364 **Figure S3:**  $^1H$ -NMR metabolites that changed following clindamycin treatment and with FMT (VA= saline-  
365 treated cultures, dashed line; VB= FMT-treated cultures, solid line). **(A)** butyrate, **(B)** acetate, **(C)**  
366 isobutyrate, and **(D)** isovalerate. The shaded grey box indicates the clindamycin-dosing time period, while  
367 the vertical dotted line indicates the day of FMT or saline dosing. SANTA analysis with Benjamini-Hochberg  
368 FDR was used to compare the following: steady state cultures to clindamycin-treated cultures, steady  
369 state cultures to post-clindamycin cultures, and FMT-treated cultures to saline treated cultures.

370 **Figure S4:** Regularized CCA (rCCA) model correlating 16S rRNA gene sequencing data (genus-level) and  $^1H$ -  
371 NMR metabolite data. **(A)** The representation of units (a.k.a. samples) for the first two canonical variates  
372 showing the correlations between variables before (grey), during (blue), and after (orange) the  
373 clindamycin-dosing period. "A" represents samples collected from VA and "B" represents samples from  
374 VB. **(B)** Correlation circle plot showing strong correlations between variables before, during, and after the  
375 clindamycin-dosing period. Metabolites are shown in blue and bacterial genera are shown in orange.  
376 *Clostridium* cluster XI (the clostridial cluster that includes *C difficile*) is shown in a black box. **(C)** The  
377 representation of units (a.k.a. samples) for the first two canonical variates showing the correlations  
378 between variables following FMT (blue) or saline (orange) treatment. "A" represents samples collected  
379 from VA (saline-treated cultures) and "B" represents samples from VB (FMT-treated cultures). **(D)**



380 Correlation circle plot showing strong correlations between variables following FMT or saline treatment.  
381 Metabolites are shown in blue and bacterial genera are shown in orange. *Clostridium* cluster XI (the  
382 clostridial cluster that includes *C difficile*) is shown in a black box.

383 **Figure S5:** 1D  $^1\text{H}$ -NMR to confirm the identity of valerate in chemostat culture supernatants. **(A)** 1D  $^1\text{H}$ -  
384 NMR spectrum of valerate standard (blue). **(B)** Overlay of 1D  $^1\text{H}$ -NMR spectrum of valerate standard (blue)  
385 with sample spectrum (red). Each peak of the valerate standard is visible in the sample spectrum. **(C)**  
386 Overlay of 1D  $^1\text{H}$ -NMR spectra of sample before (blue) and after (red) valerate spike-in. All the peaks  
387 proposed to belong to valerate increased following spike in with valerate standard (green).

388 **Figure S6:** 2D  $^1\text{H}$ -NMR to confirm the identity of valerate in chemostat culture supernatants. **(A)** Overlay  
389 of the  $^1\text{H}$ - $^1\text{H}$  COSY spectrum of valerate standard (blue) with sample spectrum (red). Each peak of the  
390 valerate standard is visible in the sample spectrum. **(B)** Overlay of the  $^1\text{H}$ - $^1\text{H}$  TOCSY spectrum of valerate  
391 standard (blue) with sample spectrum (red). Again, each peak of the valerate standard is visible in the  
392 sample spectrum.

393 **Figure S7:** Overlay of  $^1\text{H}$ - $^1\text{H}$  COSY sample spectrum (blue) and  $^1\text{H}$ - $^1\text{H}$  TOCSY sample spectrum (red) to  
394 confirm the identity of other metabolites found in chemostat culture supernatants.

395 **Figure S8:** Statistical total correlation spectroscopy (STOCSY). **(A)** 5-aminovalerate STOCSY spectrum  
396 obtained by correlating all points in the spectra with the 5-aminovalerate resonance at 3.019 ppm. Peak  
397 clusters with high correlations (\*) correspond to positions where we expected to see peaks for 5-  
398 aminovalerate. **(B)** Succinate STOCSY spectrum obtained by correlating all points in the spectra with the  
399 succinate resonance at 2.408 ppm. No other peaks had high correlations with the peak at 2.408,  
400 confirming this peak belonged to succinate.

401 **Figure S9:** Bile acids that changed following clindamycin treatment (VA= saline-treated cultures, dashed  
402 line; VB= FMT-treated cultures, solid line). **(A)** taurodeoxycholic acid (TDCA), **(B)** glycocholic acid (GCA),  
403 **(C)** glycodeoxycholic acid (GDCA), **(D)** glycochenodeoxycholic acid (GCDCA), **(E)** chenodeoxycholic acid

404 (CDCA), and **(F)** ursodeoxycholic acid (UDCA). The shaded grey box indicates the clindamycin-dosing  
405 period, while the vertical dotted line indicates the day of FMT or saline dosing. Steady state cultures were  
406 compared to clindamycin-treated cultures using SANTA analysis with Benjamini-Hochberg FDR.

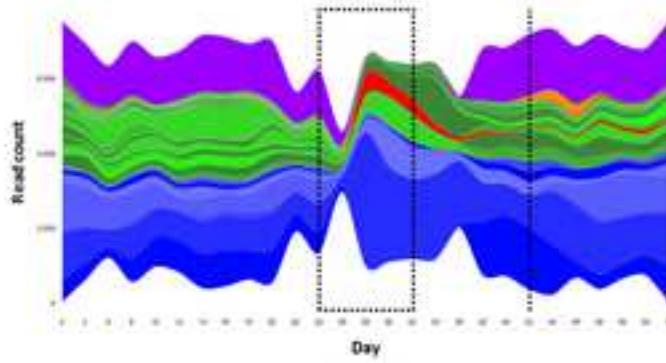
407 **Figure S10:** Regularized CCA (rCCA) model correlating 16S rRNA gene sequencing data (genus-level) and  
408 bile acid data. **(A)** The representation of units (a.k.a. samples) for the first two canonical variates showing  
409 the correlations between variables before (grey), during (blue), and after (orange) the clindamycin-dosing  
410 period. “A” represents samples collected from VA and “B” represents samples from VB. **(B)** Correlation  
411 circle plot showing strong correlations between variables before, during, and after the clindamycin-dosing  
412 period. Bile acids are shown in blue and bacterial genera are shown in orange. *Clostridium* cluster XI (the  
413 clostridial cluster that includes *C difficile*) is shown in a black box.

414 **Figure S11:** TCA is required for *C difficile* spore germination, but has no effect on *C difficile* vegetative  
415 growth. **(A)** *C difficile* spores were incubated supplemented brain heart infusion broth in the presence and  
416 absence of 1% TCA and grown overnight. There was a significant increase in *C difficile* germination in the  
417 presence of TCA (\*\*\*)  $p < 0.001$ . **(B)** *C difficile* vegetative cells were inoculated into supplemented brain  
418 heart infusion broth in the presence and absence of 1% TCA. There were no significant differences in the  
419 growth of *C difficile* in the presence or absence of TCA at any time point in the growth curve. Growth of *C*  
420 *difficile* in the broths was quantified by taking OD<sub>600</sub> measurements using a plate spectrometer. Error bars  
421 represent the mean  $\pm$  standard deviation.

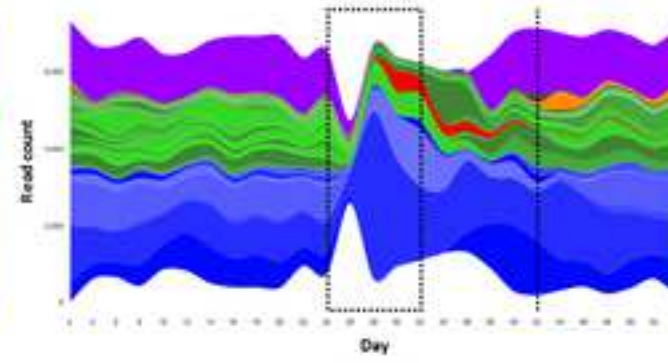
422 **Figure S12:** Schematic of key metabolite interactions with *C difficile* during health, CDI, and recurrent CDI.  
423 Initial antibiotic treatment decreases the diversity of the gut microbiota, killing bacteria that produce  
424 valerate and bile salt hydrolase (an enzyme that degrades TCA). This results in increased levels of TCA and  
425 decreased levels of valerate, allowing for *C difficile* spore germination and vegetative growth  
426 (respectively). Treatment for CDI (vancomycin/metronidazole) decreases *C difficile* vegetative cells, but *C*  
427 *difficile* spores remain and microbial community diversity remains low. Again, this antibiotic exposure

428 results in an environment with high TCA and low valerate, allowing the remaining *C difficile* spores to  
429 germinate and grow once vancomycin/metronidazole is stopped. When a patient receives FMT for  
430 recurrent CDI (usually within 1-2 days of stopping suppressive antibiotics) valerate levels (and valerate  
431 producing bacteria) and bile salt hydrolase levels (and bile salt hydrolysing bacteria) are restored, resulting  
432 in an environment that inhibits both *C difficile* germination and vegetative growth.

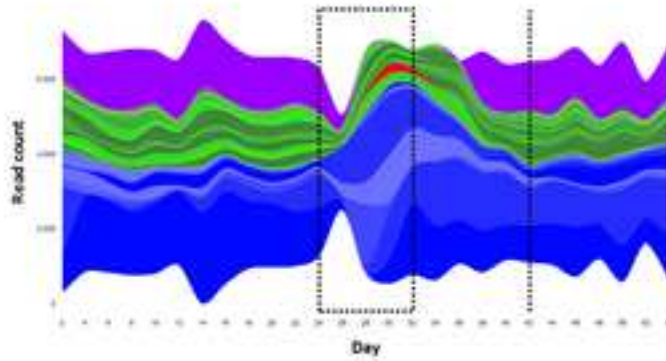
**Run 1 VA**  
(saline-treated  
cultures)



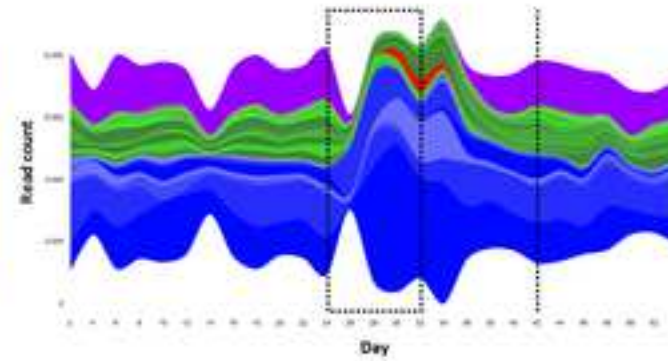
**Run 1 VB**  
(FMT-treated  
cultures)



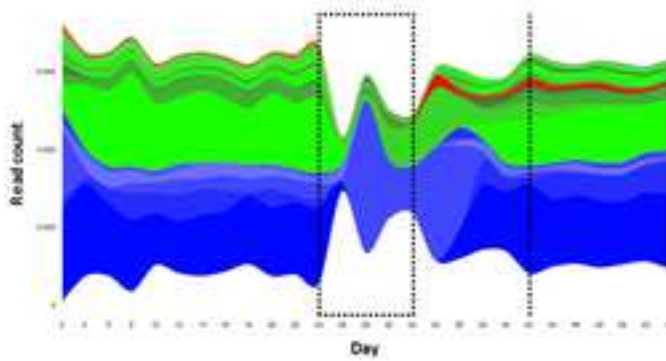
**Run 2 VA**  
(saline-treated  
cultures)



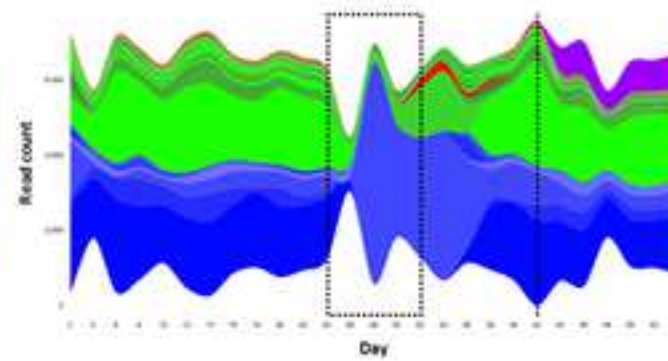
**Run 2 VB**  
(FMT-treated  
cultures)

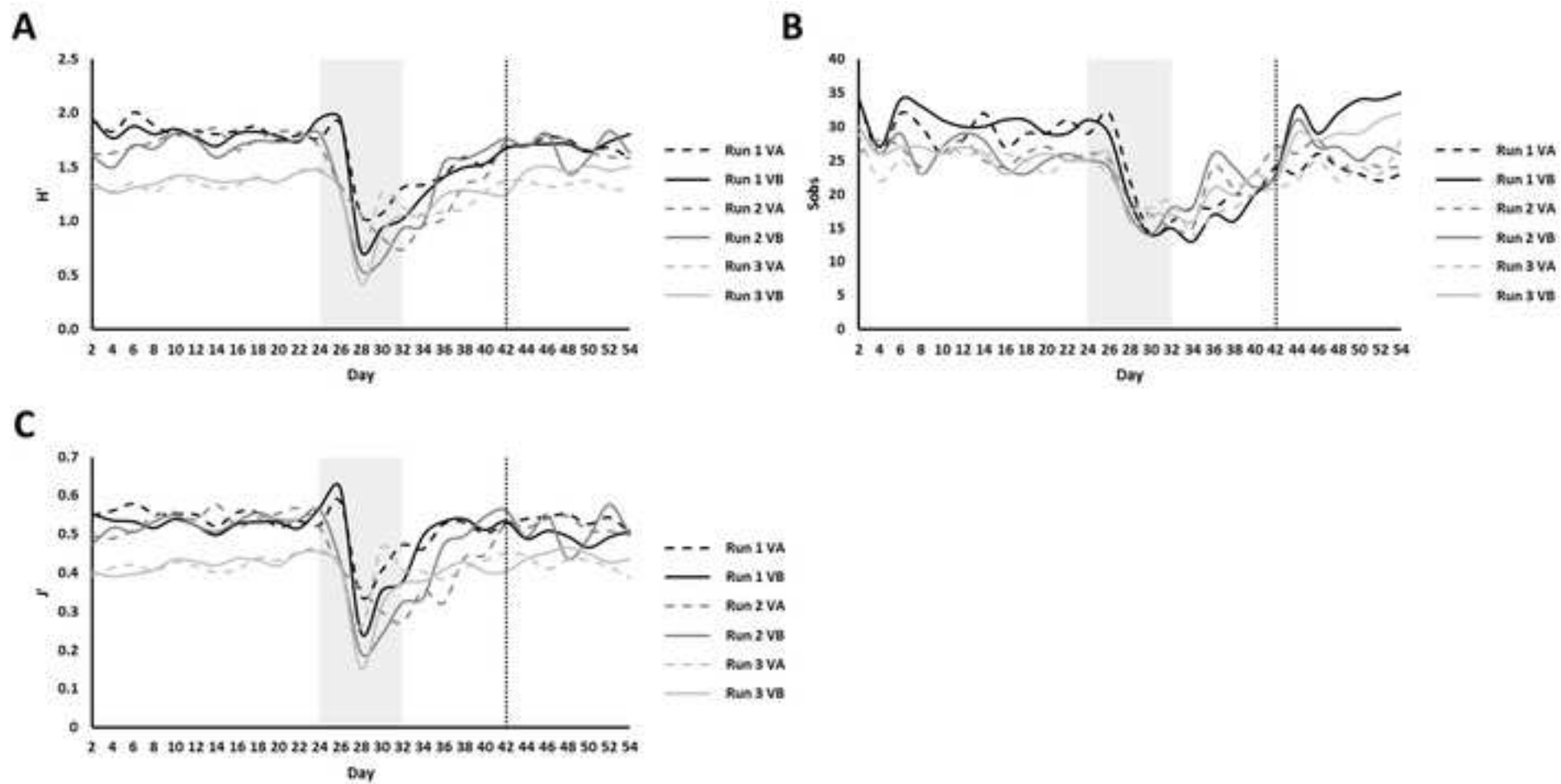


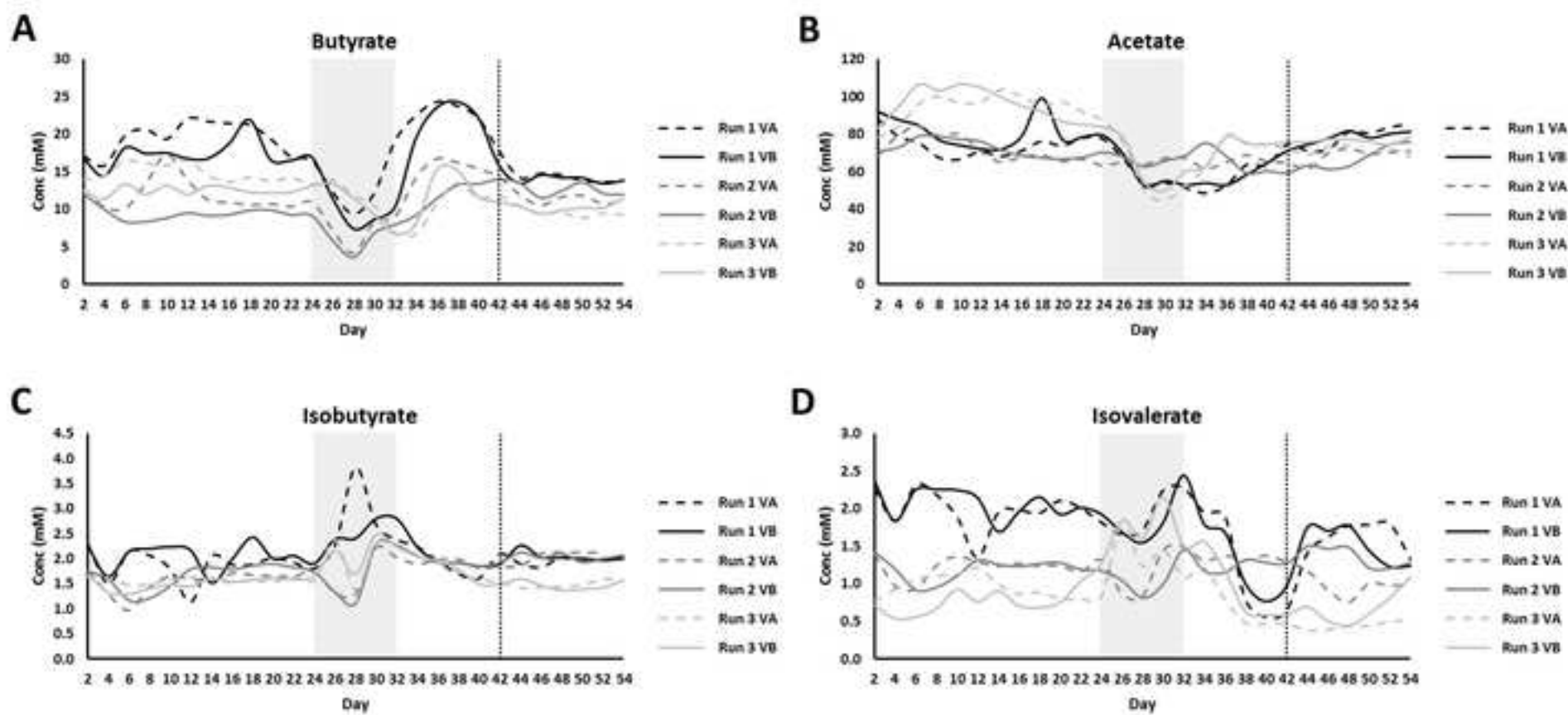
**Run 3 VA**  
(saline-treated  
cultures)

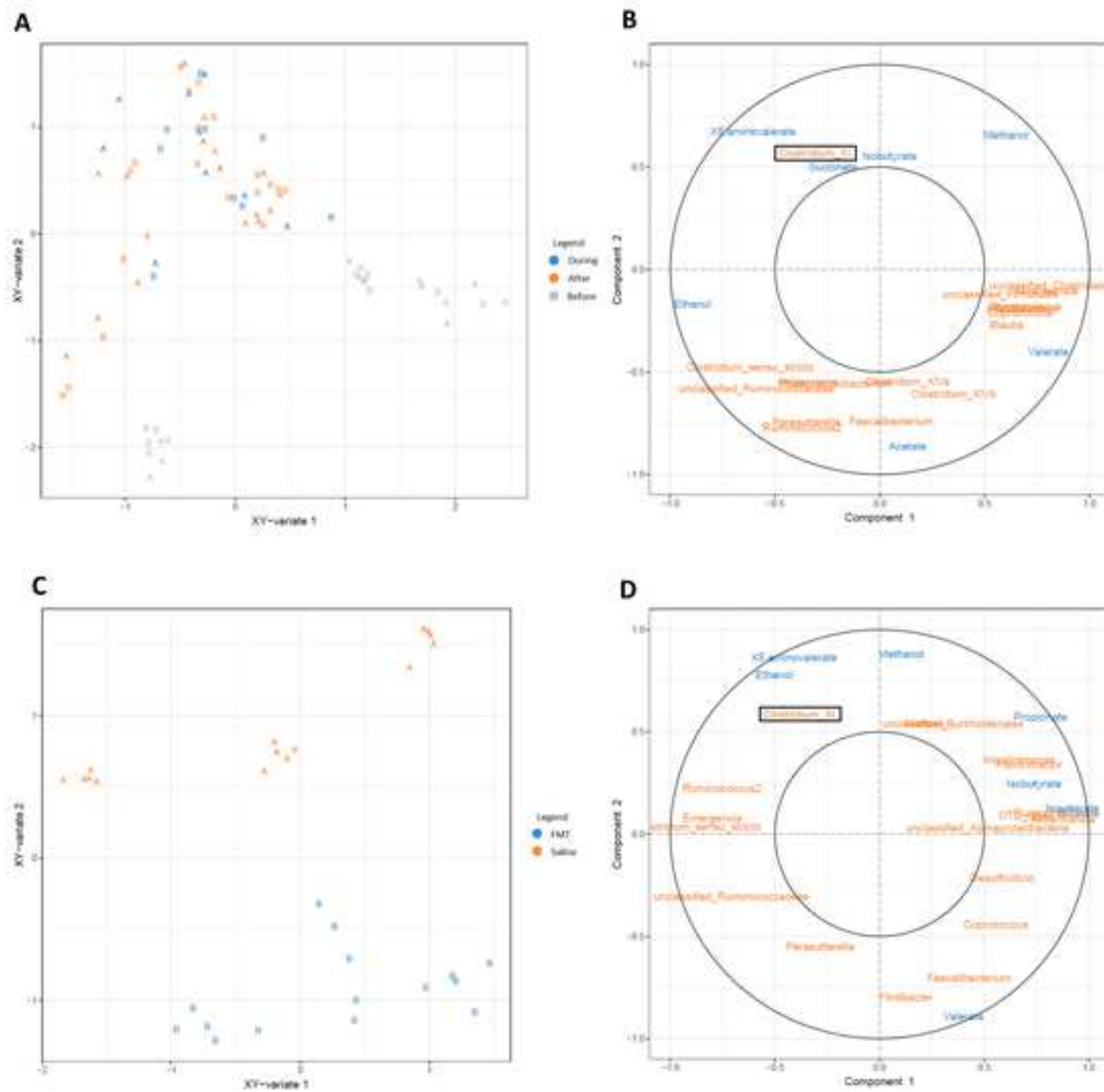


**Run 3 VB**  
(FMT-treated  
cultures)

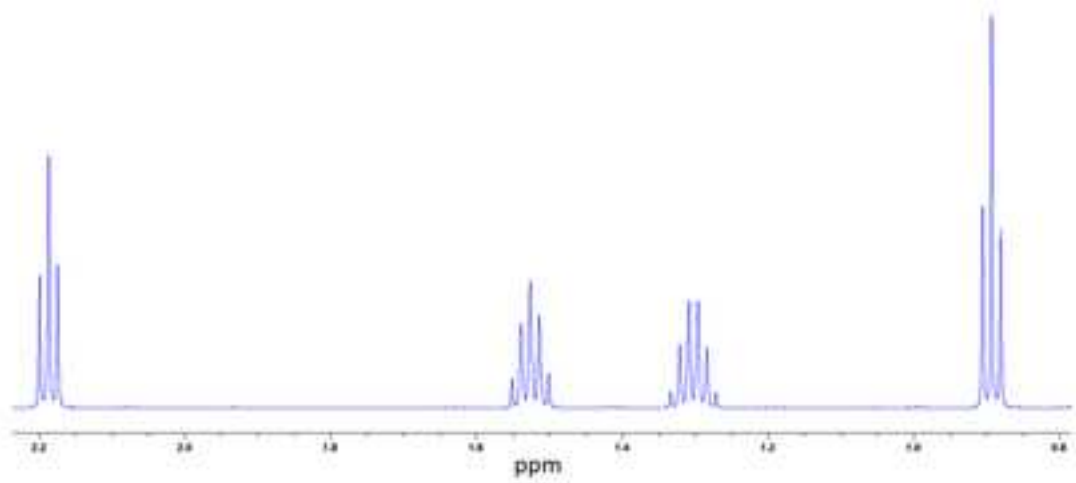
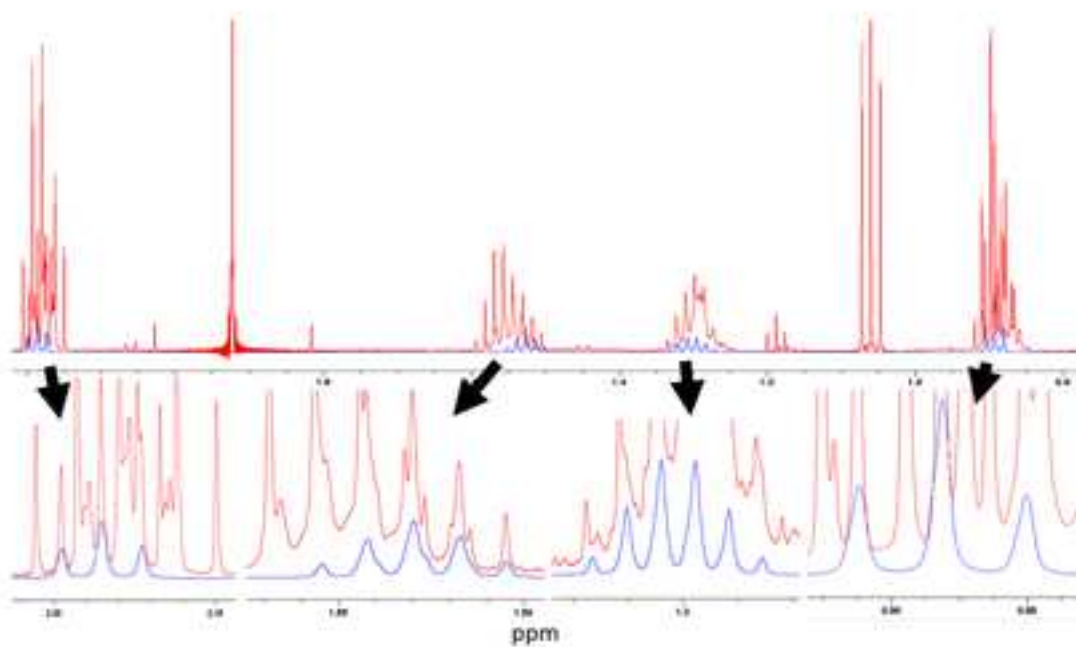










**A****B****C**